Neurons expressing trace amine-associated receptors project to discrete glomeruli and constitute an olfactory subsystem

Mark A. Johnson[a,1], Lulu Tsai[a,1], Dheeraj S. Roy[b], David H. Valenzuela[a], Colleen Mosley[c], Angeliki Magklara[c], Stavros Lomvardas[c], Stephen D. Liberles[b], and Gilad Barnea[a,2]

[a]Department of Neuroscience, Brown University, Providence, RI 02912; [b]Department of Cell Biology, Harvard Medical School, Boston, MA 02115; and [c]Department of Anatomy, University of California, San Francisco, CA 94158

Edited* by Richard Axel, Columbia University, New York, NY, and approved June 28, 2012 (received for review April 20, 2012)

Some chemoreceptors of the trace amine-associated receptor (TAAR) family detect innately aversive odors and are proposed to activate hardwired olfactory circuits. However, the wiring of TAAR neurons, the regulatory mechanisms of *Taar* gene choice, and the subcellular localization of TAAR proteins remain unknown. Here, we reveal similarities between neurons expressing TAARs and odorant receptors (ORs), but also unexpected differences. Like ORs, TAARs seem to be monoallelically expressed and localized both in cilia, the site of odor detection, and in axons, where they may participate in guidance. TAAR neurons project to discrete glomeruli predominantly localized to a confined bulb region. *Taar* expression involves different regulatory logic than *OR* expression, as neurons choosing a *Taar5* knockout allele frequently express a second *Taar* without silencing the deleted allele. Moreover, the epigenetic signature of *OR* gene choice is absent from *Taar* genes. The unique molecular and anatomical features of the TAAR neurons suggest that they constitute a distinct olfactory subsystem.

The rodent olfactory system is a powerful model for studying both learned and innate behaviors. Rodents detect a vast array of neutral odors that can be assigned behavioral relevance by learning, as well as pheromones and predator odors that stimulate instinctive responses. Thus, some olfactory circuits are highly plastic, whereas others are hardwired (1).

Odors are detected by several anatomically distinct areas in the nasal cavity that include the main olfactory epithelium (MOE), the vomeronasal organ (VNO), and the Grüneberg ganglion (2). Neurons in each one of these sensory areas project to different regions of the main and accessory olfactory bulbs (2), and the anatomical segregation between MOE and VNO persists in the projections to higher brain centers (3). The sensory neurons in the olfactory system can be further classified according to the chemosensory receptors that they express. Sensory neurons in the MOE express odorant receptors (ORs) and trace amine-associated receptors (TAARs) (4, 5). Neurons in the VNO express the two families of vomeronasal receptors (V1Rs, V2Rs) and formyl peptide receptors (2, 6, 7). Neurons that express V1Rs and V2Rs respond to different ligands, have different physical locations in the VNO, and project to different target regions of the accessory olfactory bulb (1, 8). Although TAAR and OR neurons are intermingled in the MOE, it is not known whether their axonal projections segregate to distinct anatomical regions of the olfactory bulb (OB).

Olfactory sensory neurons (OSNs) stochastically choose a single *OR* allele out of more than 2,000 possible alleles (9). We have recently shown that certain chromatin modifications are involved in *OR* silencing and that silencing occurs before *OR* expression and thus forms the foundation for *OR* choice (10). Approximately 25% of mouse *OR* genes are pseudogenes (11, 12). When a pseudogene is selected for expression, it is turned off, and the neuron switches to express another receptor gene (13–15). A mechanism by which the functional OR generates a feedback signal to stop switching has been proposed to control this process (9). Once expressed, ORs are found in cilia, where they detect odors, as well as in axons, where they instruct axon guidance (16). OSNs expressing the same OR, although randomly dispersed within a broad zone of the epithelium, project axons to two spatially invariant glomeruli in each OB (17). Second-order projection neurons called mitral cells then transmit olfactory information to several cortical and limbic areas (18). Several lines of evidence indicate that some MOE receptors mediate innate, odor-driven responses to potential mates, intruders, offspring, and predators (19, 20) and must therefore couple to hardwired neural circuits. Consistent with this notion, the projections from specific glomeruli to the cortical amygdala are more spatially concentrated and stereotyped than those to the piriform cortex (18).

TAARs belong to a distinct and evolutionarily conserved family of G protein-coupled receptors that are distantly related to biogenic amine receptors and not related to ORs. There are 15 intact *Taar* genes in the mouse, 14 of which are expressed in a dispersed pattern of OSNs similar to *OR* genes. TAAR OSNs do not coexpress other TAARs or any of the ORs examined (5). All olfactory TAARs, with the exception of TAAR6 and at least one member of the TAAR7 subfamily, are expressed in the dorsal MOE (21). Known ligands for olfactory TAARs include volatile and highly aversive amines, such as 2-phenylethylamine, a carnivore odor that repels rodents, and isoamylamine, a leucine metabolite that is avoided by mice (5, 19, 21, 22). TAARs that detect aversive odors have been proposed to activate stereotyped neural circuits. However, the projection patterns of TAAR OSNs to the OB, the subcellular localization of TAARs, and the gene choice mechanisms controlling *Taar* expression have not yet been characterized.

Here, we show that TAAR OSNs are similar to OR OSNs in some regards, but also have some unexpected and unique features. Like ORs, TAARs are localized to cilia, where they can detect odors, and also to axons. TAAR OSNs project to discrete glomeruli, but the OSNs expressing each TAAR form four to six glomeruli per bulb, whereas OR OSNs converge on only two glomeruli per bulb. Most of the TAAR glomeruli are confined to a specific region in the dorsal OB. Surprisingly, TAAR OSNs express the olfactory cell adhesion molecule (OCAM), which is predominantly expressed in OSNs that project to the ventrolateral OB (23). Examination of knockout mice in which the coding sequence of *Taar5* is replaced by *LacZ* suggests that TAARs are expressed monoallelically and that neurons choosing the deleted allele reselect another *Taar* with ~50% frequency. Remarkably, unlike switching from expression of an *OR* pseudogene, the reselection of another *Taar* does not involve shutting off the original pseudogene, indicating that the mechanisms of switching and perhaps of receptor choice are distinct in TAAR OSNs.

Author contributions: M.A.J., S.L., S.D.L., and G.B. designed research; M.A.J., L.T., D.S.R., D.H.V., C.M., and A.M. performed research; M.A.J., L.T., D.S.R., C.M., A.M., S.L., S.D.L., and G.B. analyzed data; and S.L., S.D.L., and G.B. wrote the paper.

The authors declare no conflict of interest.

*This Direct Submission article had a prearranged editor.

[1]M.A.J. and L.T. contributed equally to this work.

[2]To whom correspondence should be addressed. E-mail: gilad_barnea@brown.edu.

This article contains supporting information online at www.pnas.org/lookup/suppl/doi:10.1073/pnas.1206724109/-/DCSupplemental.

Consistent with this notion, we found that the epigenetic hallmarks of *OR* gene choice are not found on *Taar*s. Taken together, our observations suggest that the TAAR OSNs constitute a distinct olfactory subsystem.

Results

TAARs Are Expressed on the Dendrites of OSNs. To reveal the subcellular localization of TAARs within OSNs, we generated antibodies against three members of the murine family (TAAR4, TAAR5, and TAAR6). We validated antibody specificity by staining HEK293 cells transfected with expression vectors bearing *Taar4*, *Taar5*, or *Taar6* (Fig. S1*A*) and by staining histological sections from the MOE in conjunction with FISH using specific cRNA riboprobes (Fig. S1 *B–D*). Each antibody labeled only HEK293 cells transfected with the appropriate plasmid and OSNs marked by the corresponding cRNA riboprobe.

Histological staining experiments with the three antibodies revealed nonoverlapping populations of OSNs in broad zones in the MOE (Fig. 1). As revealed by previous RNA FISH experiments (5, 21), TAAR4 and TAAR5 neurons are found in the dorsal area of the MOE, whereas TAAR6 neurons are located more ventrally (Fig. 1 *A*, *C*, and *E*). The frequencies of OSNs expressing individual TAARs resemble those of ORs (Fig. S2). Furthermore, subcellular analysis indicated that like ORs (16), these three TAARs are highly expressed on the dendrites of OSNs and in perinuclear compartments likely corresponding to the endoplasmic reticulum and Golgi apparatus (Fig. 1). The high levels of dendritic expression strongly support the proposed role for TAARs as bona fide receptors for volatile amines in the environment.

Axons of TAAR Neurons Converge on Distinct Glomeruli. To test whether OSNs expressing a given TAAR converge on particular glomeruli, we performed antibody staining of OB histological sections. Each TAAR antibody stained four to six glomeruli within the dorsal part of each bulb (Fig. 2 *A–C*), with some glomeruli occupying a medial position whereas others are slightly more lateral. Costaining experiments with antibodies against TAAR4 and TAAR5 revealed some adjacent but distinct glomeruli (Fig. 2 *D–F*). These results indicate that neurons expressing TAARs converge on distinct glomeruli like those expressing ORs. However, we observed more variability in the exact positions and numbers of the TAAR glomeruli than is the case with OR glomeruli (Fig. 2 *G–K* and Fig. S3). We have not detected consistent differences in the positions or numbers of glomeruli between males and females (Fig. S3).

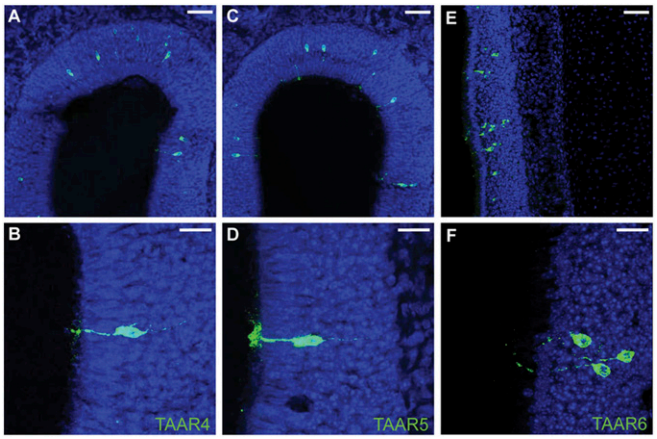

Fig. 1. TAARs are highly expressed on dendrites. Sections of MOE were stained with antibodies against TAAR4 (*A* and *B*), TAAR5 (*C* and *D*) or TAAR6 (*E* and *F*). Antibodies against TAAR4 and TAAR5 recognized distinct OSN populations in the dorsal MOE (*A* and *C*). TAAR6+ OSNs are more ventral in the MOE (*E*). High levels of staining are observed on dendrites and in perinuclear structures. Scale bars, 50 μm *A*, *C*, and *E*; 20 μm *B*, *D*, and *F*.

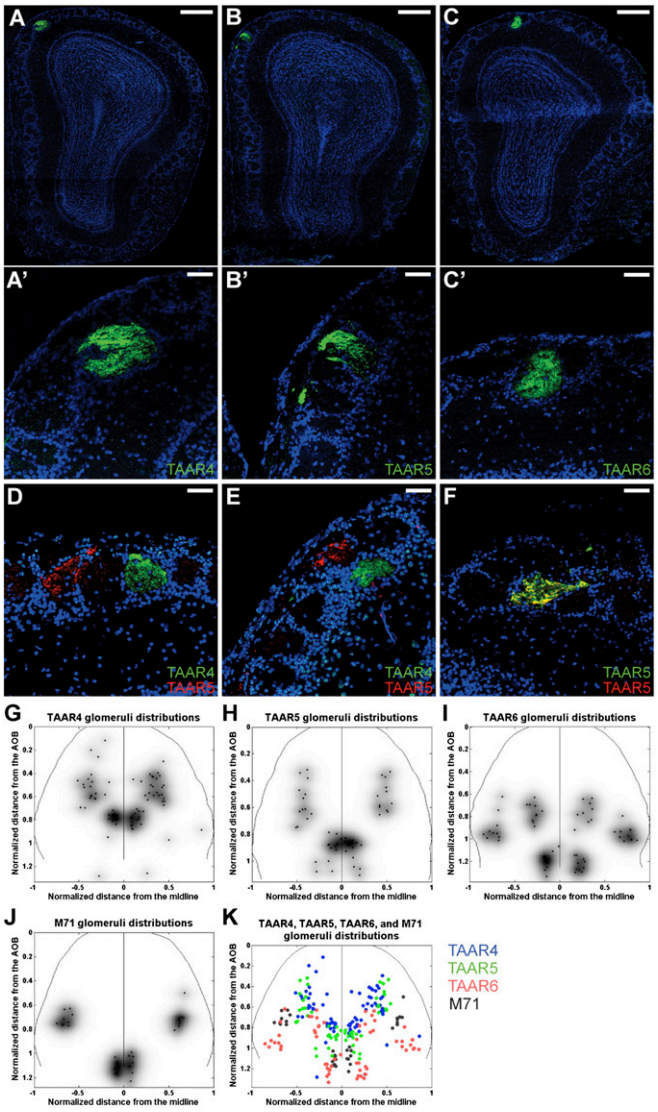

Fig. 2. TAAR neurons project to distinct glomeruli. Sections of OB were stained with antibodies against TAAR4 (*A* and *A′*), TAAR5 (*B* and *B′*), or TAAR6 (*C* and *C′*). Each antibody recognized a distinct group of glomeruli. We show representative glomeruli for each TAAR. (Scale bars, 300 μm in *A–C*; 50 μm in *A′–C′*.) (*D* and *E*) Costaining with rabbit antisera against TAAR5 (red) and guinea pig antisera against TAAR4 (green) demonstrates that OSNs expressing different TAARs project to adjacent but nonoverlapping glomeruli. (*F*) Rabbit (red) and guinea pig (green) antisera against TAAR5 label the same glomerulus. (Scale bars, 50 μm.) (*G–J*) Smoothed density plots for the glomeruli of TAAR4 (*G*), TAAR5 (*H*), TAAR6 (*I*), and M71 (*J*). The normalized distance from the AOB is presented on the *y* axis (1 is the anterior tip of the AOB). The normalized distance from the midline is presented on the *x* axis (0 is the boundary between the two bulbs). (*K*) Composite distribution of all TAAR4, TAAR5, TAAR6, and M71 glomeruli. Blue, TAAR4; green, TAAR5; red, TAAR6; black, M71.

Neurons Choosing a *Taar5*-Deletion Allele Reselect Other *Taars*. We next analyzed MOE from mice carrying a modified allele ($Taar5^{LacZ}$) in which the coding sequence of *Taar5* is deleted and replaced by *LacZ*, which encodes the enzyme β-galactosidase (β-gal). In these mice, neurons that select the modified allele ($Taar5^{LacZ}$) express β-gal instead of TAAR5. We analyzed histological MOE sections from $Taar5^{LacZ/+}$ animals (Fig. 3 *A* and *B*) by two-color RNA FISH using a probe for *LacZ* (red), which

identifies the modified allele and probes for various *Taars* and *ORs* (green). As a control, two *LacZ* probes (green and red) labeled identical OSNs (Fig. 3*A*). We found populations of *LacZ*+ OSNs that were colabeled by each of eight different *Taar* probes (Fig. 3*B*), with frequencies that ranged from 2.5% (*Taar3*) to 10% (*Taar9*). Probes for *Taar7a* and *Taar8a* recognize multiple members of the corresponding *Taar* subfamilies. Combining the frequencies of reselection of all *Taars* indicates that ~50% of the OSNs that initially chose the $Taar5^{LacZ}$ allele reselected another *Taar*. For comparison, intact *Taar* genes are not coexpressed in the same neurons in WT animals (5). Interestingly, we obtained evidence that *LacZ*+ neurons can reselect *Taar5*. Most *LacZ*+ neurons (220 of 228) were negative for *Taar5*, consistent with the notion that like *ORs*, *Taar5* is expressed monoallelically in these neurons. The intensity of signal with *Taar5* was equivalent to that of other probes. Other *LacZ*+ neurons (8 of 228) were colabeled with *Taar5*, revealing that *Taar* reselection can occur in trans, like *OR* switching (13), and that there is no preferential reselection of *Taar5* among *Taar* genes. In an attempt to account for the remaining 50% of *LacZ*+ neurons, we probed for five different *ORs* that are expressed in the *Taar5* zone of the MOE and with a degenerate probe that recognizes multiple *ORs* (Fig. S4). We observed no overlapped cells (0 of 503) for four *OR* probes, ~1% overlapped cells (2 of 194) for the fifth, and ~1% overlapped cells (2 of 187) for the degenerate *OR* probe. Thus, neurons expressing the $Taar5^{LacZ}$ allele exhibit a strong bias to reselect a second *Taar*.

As expected, when we stained MOE sections from $Taar5^{LacZ/LacZ}$ mice with antibodies against β-gal and TAAR5, we observed β-gal+ but not TAAR5+ neurons (Fig. 3*C*). Costaining of MOE sections from $Taar5^{LacZ/+}$ mice with antibodies against β-gal and TAAR4, TAAR5, or TAAR6 revealed some β-gal+ OSNs that were also positive for each of the three TAARs, indicating that reselection of a new *Taar* allele results in stable protein expression (Fig. 3 *D*–*F*).

Expression of the *Taar5*-Deletion Allele Persists After Reselecting Other *Taars*. To examine whether the $Taar5^{LacZ}$ allele is turned off in neurons that reselect other *Taars,* we stained whole-mount preparations of OBs from 7-mo-old $Taar5^{LacZ/LacZ}$ mice with X-gal. Surprisingly, expression of the deleted allele persists, and neurons that express it innervate many glomeruli in a dorsal band in the OB (Fig. 4*A*). This is in stark contrast to what is observed in mice bearing an equivalent allele of an *OR* gene. In mice bearing the $P2^{LacZ}$ allele, the number of *LacZ*+ OSNs significantly diminishes with time, and the β-gal+ fibers do not converge on the P2 glomerulus (24). The decrease in β-gal+ fibers is due to shut off of the deleted P2 allele (13). We further confirmed the persistence of expression from the $Taar5^{LacZ}$ allele by RT-PCR experiments that revealed that whereas the message of a deleted *OR* allele shut off, the deleted *Taar* allele continued to be expressed in the MOE of adult mice (Fig. S5).

We then costained histological sections from the OBs of $Taar5^{LacZ/+}$ mice with antibodies against β-gal and TAAR4 (Fig. 4*B*), TAAR5 (Fig. 4*C*), or TAAR6 (Fig. 4*D*). Consistent with the whole-mount staining results, we observed multiple β-gal+ glomeruli spread over a dorsal band in the OB. For each one of the three receptors examined, we observed glomeruli that receive β-gal+ fibers. Thus, expression of *Taar* alleles persists even in the absence of a full-length TAAR, unlike *OR*s, where the production of full-length protein is necessary for maintaining the transcriptional stability of a chosen allele (13–15). OSNs that initially choose the $Taar5^{LacZ}$ allele reselect another receptor with a strong bias toward other *Taars* and continue to express the original allele. Furthermore, OSNs that reselect a new *Taar* incorporate into the neural circuit of the new receptor.

Unlike the Dorsal OR Glomeruli, the TAAR Glomeruli Express OCAM. The cell adhesion molecule OCAM labels the axons of OR OSNs that converge on glomeruli in the ventrolateral OB (23). OCAM is believed to participate in the initial sorting of the axons destined to these glomeruli from the axons heading to the dorsomedial portion of the OB (25). To molecularly define the portion of the OB where

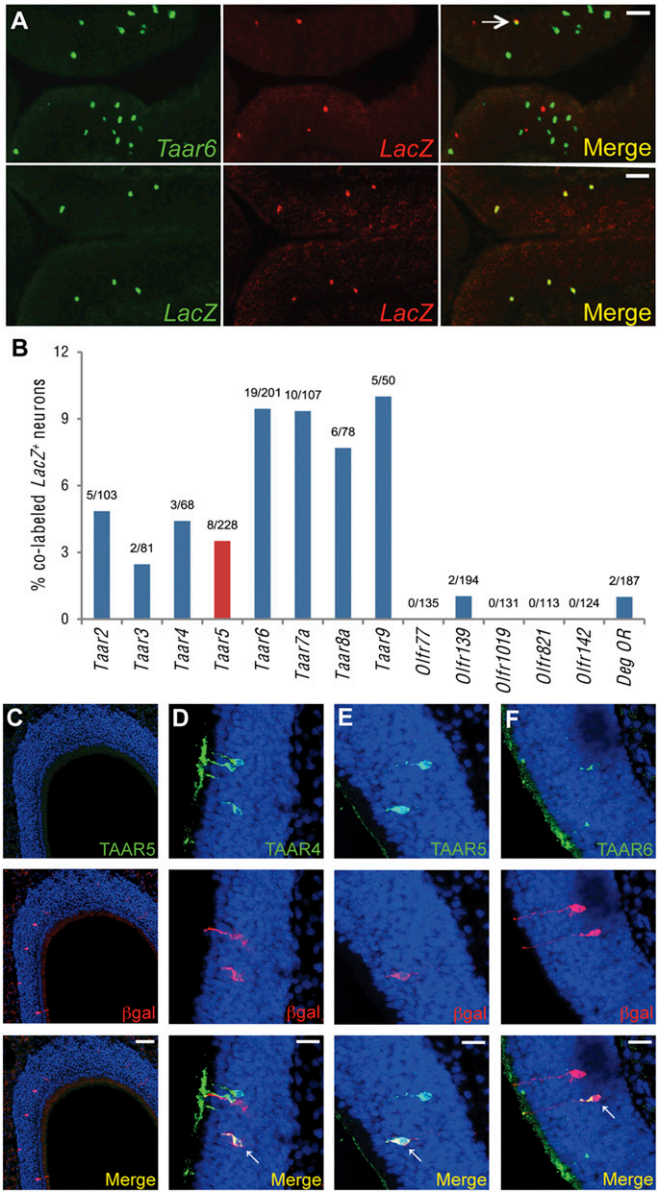

Fig. 3. OSNs that choose a deleted *Taar5* allele predominantly reselect other *Taars*. MOE sections from mice that have the *Taar5* coding sequence replaced by *LacZ* ($Taar5^{LacZ}$) were analyzed by two-color RNA FISH and by immunostaining. Except where indicated, $Taar5^{LacZ/+}$ animals were analyzed in all experiments. (*A*) A representative two-color RNA FISH experiment with probes for *Taar6* (green) and *LacZ* (red) reveals distinct but overlapping populations of OSNs. The arrow marks a cell labeled by both probes. In a control experiment, two probes for *LacZ* (green and red) label the same OSNs. (*B*) Compilation and quantification of two-color RNA FISH experiments with probes for *LacZ* and for the various *Taars* or *ORs* (including a degenerate probe that detects multiple *ORs*), as indicated. The bars represent the percentage of *LacZ*+ neurons that were also labeled by the probe for each receptor, with specific cell counts indicated above. The red bar indicates neurons that are positive for *Taar5* and for *LacZ* (indicating switching to the WT allele of *Taar5*). Note that the probes for *Taar7a* and *Taar8a* recognize the entire respective *Taar* subfamily. (Scale bars, 100 μm.) (*C*) MOE of $Taar5^{LacZ/LacZ}$ stained with antibodies against TAAR5 (green) and β-gal (red). As expected, no signal is observed with the antibody against TAAR5. (Scale bar, 100 μm.) (*D*–*F*) MOE sections of $Taar5^{LacZ/+}$ were costained with antibodies against β-gal (red in all three panels) and TAAR4 (green in *D*), TAAR5 (green in *E*), or TAAR6 (green in *F*). Arrows in the Merge panels mark OSNs coexpressing β-gal and the corresponding receptors, indicating OSNs that reselected a new TAAR. (Scale bars, 50 μm.)

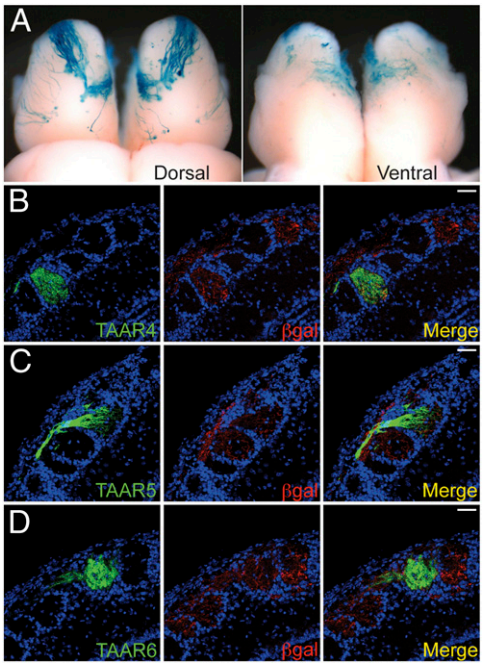

Fig. 4. Expression of the *Taar5*-deletion allele persists after selecting another *Taar*. (*A*) X-gal staining of whole-mount preparations of OB from 7-mo-old $Taar5^{LacZ/+}$ mice. Both dorsal and ventral views are presented. (*B–D*) Costaining of OB sections from $Taar5^{LacZ/+}$ mice with antibodies against β-gal (red in all panels) and TAAR4 (green in *B*), TAAR5 (green in *C*), and TAAR6 (green in *D*). β-gal+ axons are observed in glomeruli for each TAAR. (Scale bars, 50 μm.)

the TAAR glomeruli are located, we costained bulbs from adult WT mice with antibodies against OCAM and TAAR4, TAAR5, or TAAR6. To reveal all of the glomeruli, we also stained with antibodies against the vesicular glutamate transporter VGLUT2. As expected, most OCAM+ glomeruli are located in the ventrolateral portion of the OB. However, a small population of dorsomedial glomeruli and the axonal bundles that innervate them are also OCAM+. To our surprise, the TAAR4, TAAR5, and TAAR6 glomeruli were all among the OCAM+ ones (Fig. 5 *A–C*). Staining of OBs from $Taar5^{LacZ/+}$ mice with antibodies against OCAM and β-gal revealed that the β-gal+ fibers innervated only OCAM+ glomeruli, suggesting that expression of OCAM is a general feature of TAAR OSNs (Fig. 5*D*).

Unlike the *OR* Gene Clusters, the *Taar* Cluster Is Not Covered by Repressive Heterochromatic Marks. The observation that deletion of the coding sequence of *Taar5* does not affect the transcriptional stability of the mutant allele raises important questions regarding the molecular differences between the regulation of expression of *OR*s and *Taar*s. We have recently shown that *OR*s undergo an unusual heterochromatic silencing before *OR* activation and that the chosen *OR* allele is free from the trimethyl marks found on lysine 9 of histone H3 and lysine 20 of histone H4 (H3K9me3 and H4K20me3, respectively) (10). Because our genetic data suggest a different regulatory logic behind *OR* and *Taar* choice, we examined whether this could be a reflection of the epigenetic state of *Taars* in the MOE. Analysis of the data collected in our previously described whole-genome ChIP-on-chip experiments (10) with a focus on chromosome 10, the chromosome where the *Taar* genes are clustered, shows that *Taars* are indeed devoid of both H3K9me3 and H4K20me3 in chromatin preparations from the MOE, whereas *OR* genes located on chromosome 10 have high levels of both modifications (Fig. 6 *A* and *B*). To verify the whole-genome analysis, we performed ChIP–quantitative PCR (qPCR) analysis using chromatin prepared from the MOE and measured the enrichment of H3K9me3 and H4K20me3 on *Taar1*, *Taar3*, and *Taar5* in this tissue. In agreement with our ChIP-on-chip data, the three *Taar* genes are devoid of these modifications (Fig. 6 *C* and *D*).

To further assess whether epigenetic silencing is involved in the transcriptional repression of *Taars*, we tested whether two other heterochromatin marks, dimethyl on lysine 9 of histone H3 (H3K9me2) and trimethyl on lysine 27 of histone H3 (H3K27me3) are enriched on these genes. H3K9me2 is found on *OR* genes in the stem cells of the MOE (HBCs) but is converted to H3K9me3 in the cells that commit to the neuronal lineage of this tissue. The levels of H3K9me2 on *Taars* are very low compared with our positive control (*Wnt2*), suggesting that this modification is also absent on these genes in the MOE (Fig. 6*E*). Finally, we examined whether *Taars* are subject to a Polycomb-mediated repression like other clustered and developmentally regulated genes (i.e., *Hox* genes). H3K27me3 is considered an accurate epigenetic imprint for Polycomb repression, but this mark is also absent from the *Taars* tested (Fig. 6*F*). In conclusion, our ChIP-on-chip and Chip-qPCR analyses for all of the known repressive epigenetic marks have not revealed any evidence for an epigenetic silencing of *Taar* genes in the MOE.

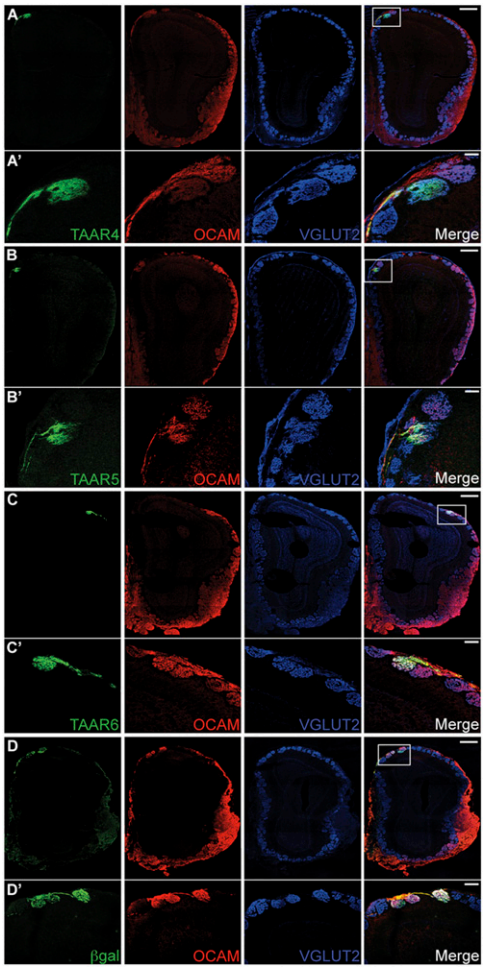

Fig. 5. TAAR glomeruli express the cell adhesion molecule OCAM. OB sections from WT (*A–C*) or $Taar5^{LacZ/+}$ mice (*D*) were stained with antibodies against OCAM (red), the presynaptic marker vesicular glutamate transporter VGLUT2 (blue), and TAAR4 (green in *A* and *A′*), TAAR5 (green in *B* and *B′*), TAAR6 (green in *C* and *C′*), or β-gal (green in *D* and *D′*). *A′–D′* represent high-magnification images of the regions contained in the white boxes in the corresponding low-magnification panels (*A–D*). In all cases costaining of OCAM and the various TAARs or β-gal is observed. Note that OCAM+ fibers innervate a cluster of dorsal glomeruli that include the TAAR glomeruli. (Scale bars, 300 μm in *A–D*; 50 μm in *A′–D′*.)

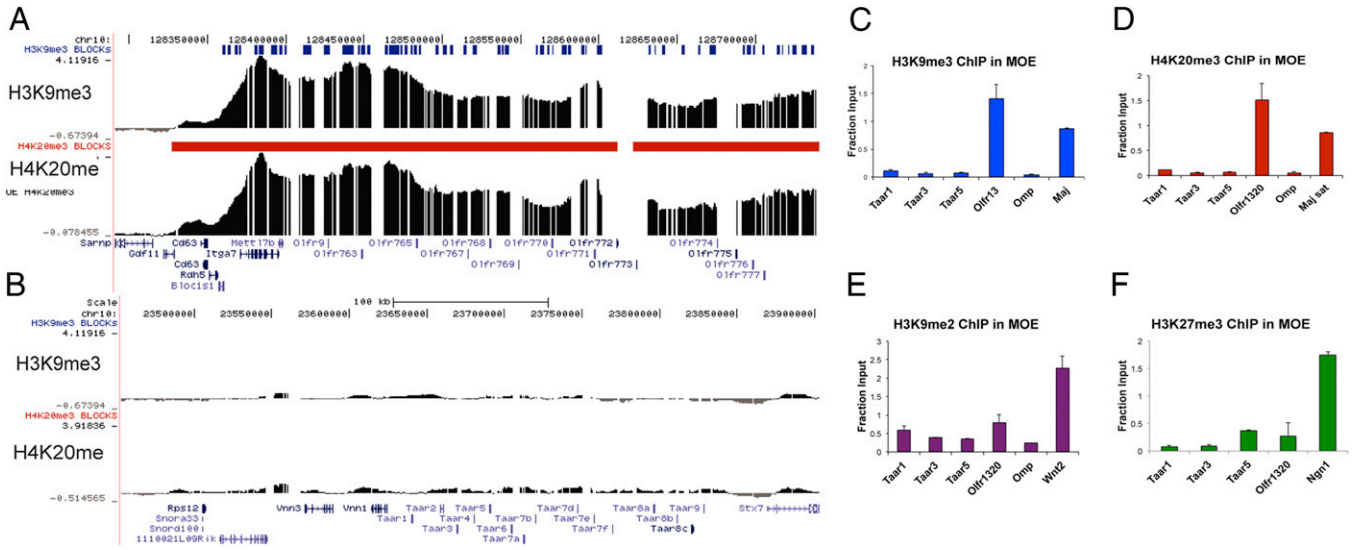

Fig. 6. *Taar* cluster is not covered by repressive heterochromatic marks. (*A* and *B*) ChIP-on-chip experiments for H3K9me3 and H4K20me3 in the MOE as previously described (10). (*A*) Part of an *OR* cluster on chromosome 10. The blue (H3K9me3) or red (H4K20me3) bars represent significant peaks (false discovery rate ≤5%) identified by model-based analysis of 2-color arrays using parameters: window = 10 kb, minimum number of probes = 20, and maximum gap = 1 kb. The black bars represent the enrichment of signal hybridization intensity over input DNA. (*B*) The *Taar* cluster, also on chromosome 10, is devoid of H3K9me3 or H4K20me3. (*C–F*) ChIP-qPCR analysis using native chromatin preparations from the MOE with various antibodies for repressive chromatin marks. In each case different genes serve as positive controls, and *Omp* is used as a negative control as indicated. The gene *Olfr1320* is shown here as a representative *OR*. Values are the mean of duplicated qPCR. Error bars indicate SEM. (*C*) H3K9me3 ChIP-qPCR and (*D*) H4K20me3 ChIP-qPCR. Both *Olfr1320* and major satellite repeats (Maj sat) serve as positive controls (10). (*E*) H3K9me2 ChIP-qPCR. *Wnt2*, which is not particularly enriched on *OR*s from a whole MOE preparation (10), serves as a positive control. (*F*) H3K27me3 ChIP-qPCR. *Neurogenin1*, a developmentally regulated gene in the MOE, serves as a positive control. The *OR* clusters do not exhibit Polycomb-mediated repression (10).

These observations strongly suggest that different mechanisms control *OR* and *Taar* gene choice.

Discussion

Most of the odors that rodents detect acquire valence through experience that involves learning and association. Some odors, however, elicit innate and stereotyped behavioral responses toward members of the same species (pheromones) or other species (kairomones and allomones). Several lines of evidence suggest that some pheromones and kairomones are detected by OSNs in the MOE and not only by neurons in the VNO (19–21). The activation of some neurons in a broad dorsal area of the MOE is implicated in innate odor avoidance responses (19). The ligands for olfactory TAARs include volatile and highly aversive amines (5, 19, 21). TAARs have therefore been proposed to perform specialized functions by binding specific odors that activate hardwired neural circuits and ultimately elicit stereotyped, innate behaviors. A better understanding of the specialized roles of TAARs in mediating innate behaviors requires characterization of the projections of TAAR OSNs to the OB and of the mechanisms controlling *Taar* expression.

Our results reveal that TAAR OSNs converge on distinct sets of four to six glomeruli in the dorsal portion of the OB. It is noteworthy that most OR OSNs converge on only two glomeruli in each bulb. Thus, the convergence on multiple glomeruli could be a unique feature of TAAR OSNs. Interestingly, the locations of the TAAR glomeruli are less stereotyped than the positions of OR glomeruli. The TAAR glomeruli are located in a discrete dorsal region of the OB. Remarkably, OSNs expressing TAAR6, which are mostly located in a ventral zone of the MOE, also project dorsally in the OB. This is in contrast to OR OSNs that maintain a general organization whereby OSNs located ventrally in the MOE tend to project to ventral glomeruli, and OSNs located in the dorsal zone of the MOE project dorsally in the OB (26). This observation may reflect unique properties of the "TAAR region" of the OB, such as the projections from these glomeruli further into the brain.

The projection of the ventral TAAR6-expressing OSNs to dorsal glomeruli may also indicate that the axon guidance mechanisms involved in wiring the TAAR OSNs are different from those controlling the projection of OR neurons. Consistent with this notion, the axons of TAAR OSNs express the cell adhesion molecule OCAM that is predominantly associated with OR OSNs that project to the ventrolateral part of the bulb (23). Indeed, one of the TAAR6 glomeruli is at the very dorsal end of the OCAM region of the lateral bulb (Fig. 5*C*).

Our experiments reveal that TAARs are highly expressed on dendrites, consistent with binding environmental ligands. Like ORs, TAARs are also expressed on axons, suggesting that they may participate in axon guidance in a similar manner to the mechanism proposed for ORs (16, 24). This mechanism whereby a receptor that functions primarily on the dendrite is also expressed at low levels on the axon and participates in guidance may be unique to the olfactory system. Such a dual function of receptors encoded by the nonrelated gene families of *ORs* and *Taars* could thus be an example of convergent evolution. Alternatively, this solution for the problem of axon guidance could be used in other neural circuits, and the massive convergence of axons on a glomerulus enables us to detect it.

Our results suggest that like *OR*s, *Taars* are expressed monoallelically. Furthermore, like OR OSNs, when TAAR OSNs choose an allele that does not encode a functional receptor, they allow the expression of another receptor allele. The high frequency of reselection of other *Taars* may indicate that these OSNs are dedicated to expressing *Taar*s. However, we cannot rule out that TAAR OSNs could also express certain *OR*s or perhaps other receptors. Reselection is not restricted to the adjacent genes in the cluster, although there may be a bias for genes that are downstream of *Taar5*. The high frequency of reselection of *Taar6*, which is normally expressed more ventrally than *Taar5*, indicates that the zonal restriction of *Taar* expression operates only in earlier developmental stages of the OSN. Finally, the observation that heterozygous mice turn on the other *Taar5* allele indicates that the reselection can occur in trans.

Each TAAR OSN expresses only one functional *Taar* (5). We observe that neurons expressing a *Taar*-deletion allele express a second *Taar*, consistent with a role for the *Taar* coding

sequence in preventing expression of a second receptor. Surprisingly, the expression of the *Taar*-deletion allele persists even after another gene is chosen. By contrast, OR OSNs only allow transcription of a single *OR* allele at a time, so for a new functional allele to be activated, the initially chosen pseudogene must be turned off (13–15). What we observe with *Taar*s is therefore not gene switching, but rather reselection of another *Taar* allele and permission for concomitant expression. Whereas in OR OSNs the coding sequence of the expressed *OR* is necessary both to inhibit switching to another *OR* and to stabilize receptor choice, in TAAR OSNs, the coding sequence of the expressed *Taar* inhibits the selection of another *Taar* but does not affect the stability of receptor choice.

In view of our observation that deleting the coding sequence of *Taar5* does not affect the transcriptional stability of the mutant allele, we analyzed the molecular differences between the regulation of expression of *ORs* and *Taar*s. We previously showed that *ORs* undergo an unusual heterochromatic silencing by the addition of H3K9me3 and H4K20me3 marks before *OR* activation and that the chosen allele is free from these marks (10). Examination of the *Taar* genes revealed that *Taars* are devoid of these marks, whereas *ORs* located on the same chromosome are highly enriched for them. Furthermore, our analyses for all of the known repressive epigenetic marks have not revealed any evidence for epigenetic silencing of *Taar*s in the MOE. These observations strongly suggest that different mechanisms control *OR* and *Taar* gene choice. Most *ORs* are organized in clusters on almost all of the chromosomes. By contrast, the *Taar* family forms a single cluster on chromosome 10. Our data suggest that TAAR OSNs are mostly limited to choosing *Taars*. Thus, the challenge of choosing a single allele is reduced in these OSNs, allowing for a different mechanism of receptor gene choice. In mice, 25% of *OR*s are pseudogenes (11, 12), but only *Taar7c* is a pseudogene. Thus, the burden of pseudogene selection is significantly lower in TAAR OSNs. Furthermore, if TAARs detect mostly aversive odors, there may have been less selective pressure for a mechanism to assure singular *Taar* expression. Our data regarding *Taar* reselection are reminiscent of the *Drosophila* opsins that generate a feedback signal, the absence of which allows photoreceptor neurons to express an additional opsin gene without terminating transcription of the originally selected allele (27).

Our data suggest that TAAR OSNs constitute a distinct olfactory subsystem because they differ from OR OSNs in their mechanisms of gene choice, some aspects of axon guidance, and in their projection patterns in the OB. The similarities between *Taar*s and *ORs* also raise interesting evolutionary questions. It seems that these two distinct families of chemoreceptors evolved to be expressed monoallelically in the MOE, but the mechanisms controlling singular expression seem to be different. The receptors from both families evolved to be expressed both on the dendrites of OSNs, where they function as chemoreceptors, and on their axons, where they may participate in guidance. TAAR OSNs are poised to extract specific environmental cues and participate in circuits that evoke uniform and innate responses. Our analysis of the projection patterns of TAAR OSNs in the OB may facilitate dissection of the next level of these circuits to determine whether they are indeed hardwired.

Materials and Methods

Animals. C57/Bl6 mice were purchased from Jackson Labs, and *Taar5* knockout mice were purchased live from the Knockout Mouse Project Repository. All animal procedures were in compliance with guidelines of the institutional animal care and use committees of Brown, Harvard, and University of California, San Francisco. Genotyping information is provided in *SI Materials and Methods*.

Antibody Generation. Antibodies were generated as previously described (16). Immunogen information is provided in *SI Materials and Methods*

Immunohistochemistry. All of the images shown are from tissue from adult mice. Protocol details are provided in *SI Materials and Methods*.

Two-Color RNA FISH. Two-color RNA FISH experiments were performed as described previously (6), except that hybridizations were done at 58 °C. Probe information is provided in *SI Materials and Methods*.

Glomerular Distribution Maps. Flattened 2D plots of the dorsal OB were reconstructed from coronal sections stained with antibodies against each receptor. In each plot, the top is the anterior part of the bulb, and the bottom is the posterior part. The position of the center of each glomerulus was defined as the distance from the anterior tip of the OB (*y* axis) and the distance from the midline (*x* axis). Additional details are provided in *SI Materials and Methods*.

Whole-Mount X-Gal Staining. Whole-mount preparations were dissected and stained with X-gal. Images were taken using a Nikon SMZ1500 stereomicroscope. Additional details are provided in *SI Materials and Methods*.

Epigenetic Analysis. Native chromatin preparations were performed as previously described (10). Details are provided in *SI Materials and Methods*.

ACKNOWLEDGMENTS. This work was supported by National Institute of Mental Health (NIMH) Grant 5R01MH086920 (to G.B.), by National Institute on Deafness and Other Communication Disorders (NIDCD) Grant RO3DC010273, a grant from the McKnight endowment fund for neuroscience (to S.L.), and by NIDCD Grant R01DC010155 (to S.D.L.). G.B. is a Pew Scholar.

1. Dulac C (2000) Sensory coding of pheromone signals in mammals. *Curr Opin Neurobiol* 10:511–518.
2. Stowers L, Logan DW (2010) Olfactory mechanisms of stereotyped behavior: On the scent of specialized circuits. *Curr Opin Neurobiol* 20:274–280.
3. Dulac C, Torello AT (2003) Molecular detection of pheromone signals in mammals: From genes to behaviour. *Nat Rev Neurosci* 4:551–562.
4. Buck L, Axel R (1991) A novel multigene family may encode odorant receptors: A molecular basis for odor recognition. *Cell* 65:175–187.
5. Liberles SD, Buck LB (2006) A second class of chemosensory receptors in the olfactory epithelium. *Nature* 442:645–650.
6. Liberles SD, et al. (2009) Formyl peptide receptors are candidate chemosensory receptors in the vomeronasal organ. *Proc Natl Acad Sci USA* 106:9842–9847.
7. Rivière S, Challet L, Fluegge D, Spehr M, Rodriguez I (2009) Formyl peptide receptor-like proteins are a novel family of vomeronasal chemosensors. *Nature* 459:574–577.
8. Isogai Y, et al. (2011) Molecular organization of vomeronasal chemoreception. *Nature* 478:241–245.
9. Shykind BM (2005) Regulation of odorant receptors: One allele at a time. *Hum Mol Genet* 14(Spec No 1):R33–R39.
10. Magklara A, et al. (2011) An epigenetic signature for monoallelic olfactory receptor expression. *Cell* 145:555–570.
11. Young JM, Trask BJ (2002) The sense of smell: Genomics of vertebrate odorant receptors. *Hum Mol Genet* 11:1153–1160.
12. Zhang X, Firestein S (2002) The olfactory receptor gene superfamily of the mouse. *Nat Neurosci* 5:124–133.
13. Shykind BM, et al. (2004) Gene switching and the stability of odorant receptor gene choice. *Cell* 117:801–815.
14. Lewcock JW, Reed RR (2004) A feedback mechanism regulates monoallelic odorant receptor expression. *Proc Natl Acad Sci USA* 101:1069–1074.
15. Serizawa S, et al. (2003) Negative feedback regulation ensures the one receptor-one olfactory neuron rule in mouse. *Science* 302:2088–2094.
16. Barnea G, et al. (2004) Odorant receptors on axon termini in the brain. *Science* 304:1468.
17. Mori K, Sakano H (2011) How is the olfactory map formed and interpreted in the mammalian brain? *Annu Rev Neurosci* 34:467–499.
18. Sosulski DL, Bloom ML, Cutforth T, Axel R, Datta SR (2011) Distinct representations of olfactory information in different cortical centres. *Nature* 472:213–216.
19. Kobayakawa K, et al. (2007) Innate versus learned odour processing in the mouse olfactory bulb. *Nature* 450:503–508.
20. Mandiyan VS, Coats JK, Shah NM (2005) Deficits in sexual and aggressive behaviors in Cnga2 mutant mice. *Nat Neurosci* 8:1660–1662.
21. Ferrero DM, et al. (2011) Detection and avoidance of a carnivore odor by prey. *Proc Natl Acad Sci USA* 108:11235–11240.
22. Ferrero DM, et al. (2012) Agonists for 13 trace amine-associated receptors provide insight into the molecular basis of odor selectivity. *ACS Chem Biol*, 10.1021/cb300111e.
23. Yoshihara Y, et al. (1997) OCAM: A new member of the neural cell adhesion molecule family related to zone-to-zone projection of olfactory and vomeronasal axons. *J Neurosci* 17:5830–5842.
24. Wang F, Nemes A, Mendelsohn M, Axel R (1998) Odorant receptors govern the formation of a precise topographic map. *Cell* 93:47–60.
25. Chehrehasa F, St John J, Key B (2005) The sorting behaviour of olfactory and vomeronasal axons during regeneration. *J Mol Histol* 36:427–436.
26. Miyamichi K, Serizawa S, Kimura HM, Sakano H (2005) Continuous and overlapping expression domains of odorant receptor genes in the olfactory epithelium determine the dorsal/ventral positioning of glomeruli in the olfactory bulb. *J Neurosci* 25:3586–3592.
27. Vasiliauskas D, et al. (2011) Feedback from rhodopsin controls rhodopsin exclusion in *Drosophila* photoreceptors. *Nature* 479:108–112.